Paper

The Alive-in-Range Medium Access Control Protocol to Optimize Queue Performance in Underwater Wireless Sensor Networks

Vikas Raina[1], Manish Kumar Jha[2], Partha Pratim Bhattacharya[1]

[1] *Mody University of Science and Technology, Lakshmangarh, India*
[2] *ABES Engineering College, Ghaziabad, India*

https://doi.org/10.26636/jtit.2017.112317

Abstract—Time synchronization between sensor nodes to reduce the end-to-end delay for critical and real time data monitoring can be achieved by cautiously monitoring the mobility of the mobile sink node in underwater wireless sensor networks. The Alive-in-Range Medium Access Control (AR-MAC) protocol monitors the delay of sensitive, critical and real-time data. The idea evolves as it involves reduction in duty cycle, precise time scheduling of active/sleep cycles of the sensors, monitoring the mobility of the sink node with the selection of appropriate queues and schedulers. The model for the path loss due to attenuation of electromagnetic wave propagation in the sea water is explained. The three-path reflection model evaluating reflection loss from the air-water and water-sand interfaces as a function of distance between sensors and water depth is introduced. The algorithms for effective path determination and optimum throughput path determination are elaborated. The results verify that implementation of the Alive-in-Range MAC protocol has reduced the total number of packets dropped, the average queue length, the longest time in queue, the peak queue length and the average time in queue significantly, making it relevant for critical and real-time data monitoring.

Keywords—Alive-in-Range MAC, effective path determination, mobile sink, optimum throughput path determination, underwater wireless sensor network.

1. Introduction

Unmanned underwater explorations have recently gained in popularity and are relied upon in monitoring aquatic environments (comprising ponds, lakes, rivers, oceans and reservoirs, etc.) for commercial utilization, scientific investigation and disaster prevention. An exemplary system for such a type of extensive monitoring is a network comprising hundreds of tiny autonomous, wireless sensors and vehicles distributed underwater, communicating with each other and performing collaborative tasks. They are known as underwater wireless sensor networks (UWSNs).

They augment our ability to observe and predict the aqueous environments by enabling many applications, such as tactical surveillance, assisted navigation, disaster prevention, oceanographic data collection, pollution monitoring and offshore exploration [1]. Although in the specific applications involving critical and real-time data monitoring performed for limited time periods, such as rescue and military operations, parameters like throughput, end-to-end delay, jitter and packets dropped are highly influential. The battery power available in the sensor nodes already deployed cannot be increased, but the battery power of sensor nodes intentionally deployed for the operation, as well as the amount of petrol/electricity in the autonomous underwater vehicles (AUVs) can be adjusted according to the tentative duration of the operations planned.

The low and distance-dependent bandwidth, high latency, floating node mobility, sparse deployment, high error probability, frequency dependent transmission range, 3-dimensional space and poor channel conditions lead to larger power consumption during transmissions, and thus multi-hop transmissions are not always attractive in underwater communication [1]. Therefore, the proposed AR-MAC protocol is capable of continuous monitoring of critical underwater events in a very cost-effective manner, as it utilizes relatively cheap, reduced function devices (RFDs) within the network only, avoiding multi-hop transmissions.

2. Related Work

Akyildiz *et al.* [1], [2] recognize the research challenges, mainly focusing on protocol issues, hardware issues and a cross-layer design approach for UWSNs. The elemental technology used in the physical layer of underwater acoustic sensor networks is acoustic communication, because optical signals and electromagnetic signals are unsuited due to high absorption, scattering and attenuation, respectively, in the aqueous environments. They are different from terrestrial sensor networks in many attitudes: 3-dimensional space, frequency dependent transmission range, floating node mobility, longer delay, low and distance dependent bandwidth, and many more. The propagation velocity of the acoustic waves underwater is approximately 1500 m/s and the available bandwidth over a distance of a few kilometers is up to 10 kHz [2].

Liang *et al*. [3] proposed a controlled mobile sink approach in wireless sensor networks (WSNs) to prolong the network lifetime. The least amount of time at each sojourn location of the mobile sink is calculated to minimize the packet loss and the problem is formulated as a mixed integer linear programming (MILP). The results showed the enhancement in network lifetimes, provided by various algorithms by varying the value of the total distance travel per tour.

Kartha *et al*. [4] have compared analytical models for delay performance to observe that the polling model is more effective in modeling the mobility-assisted data collection framework for UWSNs. The analytical models implemented are validated with an experimental setup developed using the NS-2 based AquaSim simulator. The outcomes illustrate that the proposed framework reveals superior performance in terms of energy efficiency, network lifetime and packet delivery ratio at the cost of increased message latency.

Sendra *et al*. [5] have performed a set of measurements of electromagnetic (EM) waves at 2.4 GHz in underwater environments. The water conditions are fixed and the behavior of EM waves as a function of several network parameters, such as the working frequency, data transfer rates and modulations, are analyzed. The output data rates are calculated at different frequencies and distances.

Elrashidi *et al*. [6] presented a comprehensive study of underwater propagation of EM waves for the WSN of 2.4 GHz. A model for the path loss due to attenuation of electromagnetic waves in sea and pure water is introduced. A bow tie antenna is used to compensate for the path loss. A reflection model is introduced to illustrate the impact of air-water and water-sand interfaces as a function of distance between sensors and water depth. The path loss is evaluated and compared as a function of resonance frequency at different distances between the sensors for pure and sea water.

Letre *et al*. [7] performed an analysis of throughput and delay of unslotted IEEE 802.15.4, offering high levels of reliability of a low power and low data rate protocol. The maximum throughput and minimum delay of the unslotted version of the protocol is analyzed at 2.4 GHz. The maximum throughput and minimum delay are calculated at different operating frequencies and at various address sizes. Finally, the comparison of bandwidth efficiency for 2.4 GHz and 868/915 MHz is performed and the minimum delay – as a function of payload size at 2.4 GHz – is evaluated.

Yu *et al*. [8] introduced a low jitter scheduling technique clarifying the dependence of TDMA scheduling for sensors, and point out the correlations between scheduling delays, overall quality control and focus on reducing jitter in scheduling. The values of normalized jitter at starting and ending time slots are evaluated.

Aoun *et al*. [9] consider the problem of modeling the transmission of real-time data from a single node of a WSN to the next hop or access point. A thresholding policy supported by an analytical model is introduced, and it is responsible for deciding whether to transmit a data packet or drop it and transmit the next one. A sensor system model, packet delivery ratio calculation and probability of an empty system are introduced. The packet delivery ratio gain with respect to the packet arrival rate is evaluated.

Liu *et al*. [10] have introduced a Doppler-assisted time synchronization scheme, where the mobile Doppler scaling factor is estimated to gather relative movement velocities of sensor nodes. A model is developed to establish the relationship between the joint and individual Doppler effects caused by sensor mobility and clock skew. The synchronization, data collection, velocity estimation, propagation delay estimation and linear regression phases are analyzed. The propagation delay with respect to velocity and clock skew is estimated. An evaluation is performed.

Yang *et al*. [11] exploit mobility of the sink node to transmit non-delay-sensitive data and avoid multi-hop transmissions. An area partitioning algorithm, a transmission mechanism based on superposition coding and a MAC protocol has been proposed. The simulation results produce optimum values of the minimum distance algorithm and the maximum throughput algorithm with respect to travel distance, transmission throughput, time spent in each group and energy consumption of the group at the different numbers of sensor nodes.

Tuan Le *et al*. [12] have approximated queuing analysis for IEEE 802.15.4 sensor networks. The objective is to optimize the number of nodes deployed with a QoS guarantee. A deployment optimization model has been proposed for the beaconless mode of operation, using the M/M/1 queuing model. Such parameters as total packet loss rate and end-to-end delay at different arrival rates and at various numbers of sinks with different data rates have been evaluated and compared between the NS-2 simulation model and the M/M/1 queuing model.

Paphitis *et al*. [13] have utilized a fluid dynamic model to estimate the queue formation rate in WSN. The precise estimation of the rate with which buffers of the nodes fill-up, can contribute to congestion control. Performance can be improved by developing a mechanism based on the estimate, to control congestion and overload. The traffic flow model, queue formation rate model and congestion triggering mechanism have been introduced. The results, such as the average received packets ratio, total energy consumption and average hop-by-hop delay at different data rates are evaluated and compared.

Mao *et al*. [14] have presented how the queueing theory is applied to evaluate the performance of WSN using queuing network models. The performance analysis has considered both kinds of data and routing packets. The proposed M/M/1/K analytical model has elaborated the coverage of signal transmission, open and closed queueing networks. The mean number of packets, mean response time and mean throughput at each sensor node for both data information and routing information networks has been evaluated.

Fan Ke *et al*. [15] have presented a method to determine the trade-off between packet transmission speed and battery life in WSNs. The important data packets have been assigned to high priority queues. A network lifetime pro-

longation approach, founded on the Priority Queue N strategy, has been proposed. The variation of probability levels in different states for different service rates with different probability of packet collision, at different queue thresholds has been evaluated. Finally, the N threshold value for the lowest power consumption value has been determined.

Vanithamani *et al*. [16] have analyzed the performance of queue-based scheduling schemes in WSNs. In the Dynamic Multilevel Priority scheduling scheme, in which each node has three levels of priority, queue and non-real time packets are assigned to the two other queues based on priority. Such parameters as end-to-end delay, average task waiting time, fairness, energy consumption and network lifetime have been evaluated as well.

Byun *et al*. [17] have proposed a control-based approach to duty cycle adaptation for WSNs. High performance has been achieved under variable traffic rates by using adaptive duty cycle control through queue management. The average queue length, delay, and power consumption, at different number of hops for the proposed algorithm, have been evaluated and compared.

Peters *et al*. [18] have examined the influence of the scheduling policy on feedback control over networks based on a hybrid communication protocol, which incorporates both contention-free and contention-based medium access. A number of scheduler-controller co-design algorithms have been compared that take both the contention-based and guaranteed parts of the protocol into account using an approximation to an infinite horizon linear quadratic cost function.

Pati *et al*. [19] have proposed a conflict-free query scheduling approach in WSNs, as conflict-free real-time query scheduling is one of the most difficult tasks. The results, such as response time for different scheduling algorithms with fixed deadlines and varying query rates, have been evaluated and compared.

Zhang *et al*. [20] have proposed scheduling with predictable link reliability for wireless networked control. Such a solution is required for wireless networked control, yet co-channel interference remains a major source of uncertainty in wireless link reliability. The Physical-ratio-k (PRK) model and PRK-S algorithm required to implement it have been introduced. The results ensured that PRK-S reduces the communication delay and increases the throughput more effectively than existing scheduling protocols. Such parameters as packet delivery reliability, settling time, median latency and throughput have been evaluated and compared for different algorithms.

Pati *et al*. [21] have proposed an Advanced Real-Time Query scheduling approach for WSNs. It works with three new schedulers: Advanced Non-Preemptive Query Scheduler, Advanced Preemptive Query Scheduler and Advanced Query Scheduler. The response time with fixed deadlines and varying query rates have been evaluated.

Peters *et al*. [22] have investigated the co-design of a scheduler and controller for feedback control over wireless industrial hybrid protocol networks. The possibilities and limitations of feedback control over hybrid networks that are based on IEEE 802.15.4 protocol are considered. The results illustrated that careful co-design of the scheduler-controller results in significant performance gains compared to round robin heuristics.

Shahid *et al*. [23] have used an improved low power scheduler for OSS-7 by implementing the open source DASH 7 stack. It has improved the performance up to 75%, on average, in terms of execution time, thus leading to reduced dynamic power consumption.

Chovance *et al*. [24] have presented a real-time scheduler in an operating system running on the ARM Cortex (M0, M3, M4) processors used in small mobile robotics, with the kernel response of around 1 ms. It can be used for WSNs due to its strong modularity, advanced sleep modes and event-driven programming capability.

Jhamshed *et al*. [25] have proposed a node-level optimal real-time priority based dynamic scheduling algorithm that schedules tasks according to their priorities, by changing the frequency with the use of dynamic voltage frequency scaling, and hence makes more efficient use of energy and helps in achieving QoS for delay sensitive traffic.

In this paper, a queuing model has been developed with a mechanism which utilizes the sink node velocity, the most suitable path with controlled mobility, low duty cycle, appropriate number of queues having optimum queue length, proper schedulers and, finally, the AR-MAC protocol has been implemented to improve network performance.

The rest of the paper is organized in the manner described below. Section 2 explains the related work. Section 3 illustrates the proposed AR-MAC protocol. Section 4 presents the preliminaries. Mathematical models are explained in Section 5. Section 6 contains an explanation of the simulation scenarios and algorithms. Sections 7 and 8 illustrate simulation results and contain their analysis. Section 9 concludes the paper and presents the future work.

3. The Alive-in-Range MAC Protocol

In AR-MAC as the sink node is continually mobile without sojourns. A centralized duty-cycle based MAC protocol is used to schedule the transmissions from the sensors. Normally, all sensor nodes are in the sleep state. As the sink traverses the most effective path, sensors coming into the range of the sink node become active and start transmissions. The maximum data transmission range equals 20 m. It is determined with respect to the effective power received at the sink node. In the example shown in Fig. 1, when the mobile sink node is at location 1, sensor nodes A and B are within range. After the sink moves into the range, sensor nodes A and B become active after sensing the beacons. At locations 2 and 3, sensors A, B, C and D are within range and become active. At position 4, sensor nodes A and B are out of range and enter the sleep mode, but nodes C and D are still active. The centralized approach to schedule active cycles eliminates collisions and reduces the synchronization

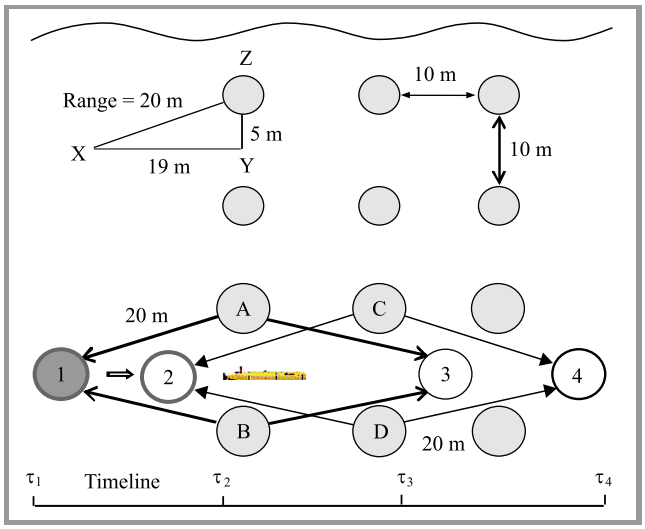

Fig. 1. Simulation architecture of the AR-MAC protocol.

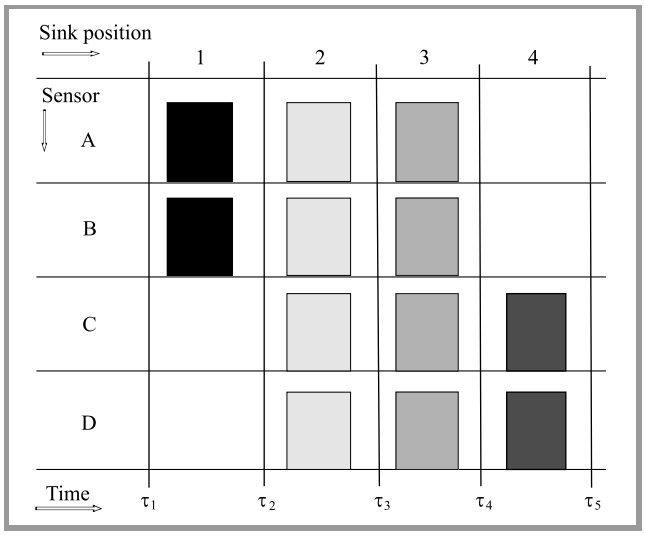

Fig. 2. The timing diagram of active and sleep scheduling in AR-MAC.

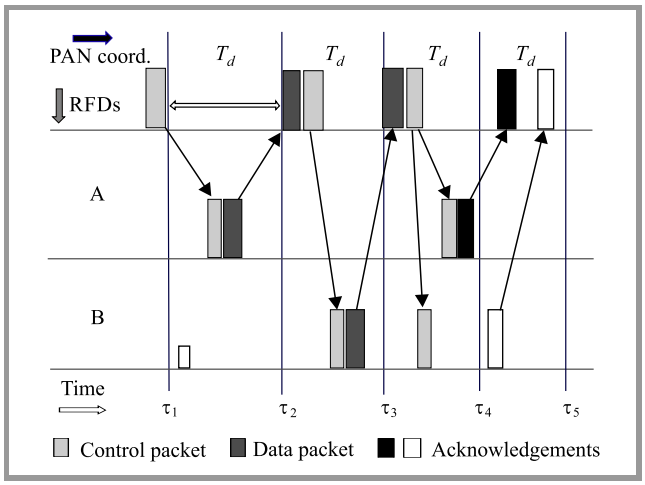

Fig. 3. The timing diagram of data transmission and reception in AR-MAC.

requirements among the sensors. Figure 2 presents the timing diagram of active/sleep scheduling. The process of data transmission and data reception of the proposed AR-MAC protocol with two sensors is shown in Fig. 3. It illustrates that, after the sink moves to the data collection position, it polls each sensor sequentially. A sensor with data to transmit does so immediately after it is polled, and, in the absence of data, sends a small packet to just acknowledge the receipt of the poll. Then the sink estimates the propagation delay for each sensor based on the measurement of the round-trip time. A sensor may be re-polled immediately if its data is not received correctly. Also, if no response is obtained in response to a poll, the sink may repeat polls subject to the limited number of retransmissions. After the uplink transmissions, the sink transmits the control messages to the sensors. The messages sent by the sink also contain the schedule according to which the sensors send back their acknowledgement packets (ACK).

In this paper an attempt has been made to optimize the queue performance by avoiding the use of relay nodes/full function devices (FFDs) to forward the data from sensor nodes acting as Reduced Function Devices (RFDs). It is achieved by using sensor nodes only for the deployment of UWSNs and by adjusting the speed of the mobile sink, so that it will collect data from all sensor nodes without the requirement of any sojourn. Moreover, the duty cycle of the sensor nodes is minimized as they become active only when the sink node is located within their transmission range. Otherwise, they are in sleep mode, which reduces energy consumption, minimizes collisions, diminishes the number of packets dropped and eliminates the formation of bottlenecks at the sink nodes.

In recent research, there are several bottleneck constraints affecting the mobility of a sink for the enhancement of network performance. These constrictions include the maximum distance between two consecutive movements, the maximum number of sojourn locations and the minimum sojourn time at each sojourn location. The distance-constrained mobile sink problem is dulled by controlling the mobility and by finding the most suitable path for the sink node to traverse the sensor network. The mobility of a sink node is beneficial for better balancing of energy consumption among the sensors.

4. Preliminaries

The preliminaries are as follows:

- an underwater wireless sensor network $U(S,E)$ is deployed comprising of n static sensors and a mobile sink, where S is the set of sensors and E is the set of radio links,
- there is no link between two static sensors as all the immobile sensors are RFDs,
- the sink and the sensor node are able to communicate if they are within the communication range of each other,

- the energy consumed by all communication operations is considered,
- it is assumed that by using radio positioning techniques, the sink is aware of the location of the sensors,
- all sensors have the same data generation rate r,
- the mobile sink offers a limited amount of energy which is sufficient for the completion of the monitoring operation, compared to the energy capacity of sensors,
- there is no sojourn location of the mobile sink, as it is moving continuously.

5. Network Models and Assumptions

5.1. Underwater Electromagnetic Wave Propagation

Conductivity, density and permittivity of water are different from and higher than those of air [17], [18]. Water differs from the air, as it has higher conductivity, higher density and higher permittivity. The value of relative permittivity of pure water is $\varepsilon_r = 79$, density is 1000 kg/m^3 and tangent loss is $\varepsilon_t = 0.924$ at 2.4 GHz. In the case of sea water $\varepsilon_r = 80.4$, density is 1033 kg/m^3 and $\varepsilon_t = 1.527$ at 2.4 GHz. The concentration of salt in the sea water determines the value of relative permittivity, which is normally 3%. In this paper the simulations are carried out for sea water only. Electromagnetic waves experience a very high path loss in underwater propagation. The Friis equation introducing the value of power received, in terms of transmitter and receiver antenna gains, transmitted power and path loss at the receiver, is expressed by the following formula:

$$\Psi_r = \Psi_i + G_i + G_r - \Theta_{path}\,, \tag{1}$$

where the gain of the transmitter and receiver antennas is denoted as G_t and G_r, the received power is Ψ_r, the transmitted power is Psi_t and the underwater path loss is Θ_{path}. All units are dBm. The expression for path loss (in dB) is:

$$\Theta_{path} = \Theta_0 + \Theta_m + \Theta_a\,. \tag{2}$$

The path loss in the air is denoted as Θ_0 and formulated as:

$$\Theta_0 = 20\log\frac{4\pi df}{\mathrm{c}}\,, \tag{3}$$

where c the speed of light in the air (m/s), the distance between transmitter and receiver in meters is denoted by d, the operating frequency is symbolized as f.
The path loss due to change in propagation medium Θ_m is:

$$\Theta_m = 20\log\frac{\lambda_0}{\lambda}\,, \tag{4}$$

where the wavelength of the signal in the air is signified as λ_0 and calculated as $\lambda_0 = \dfrac{\mathrm{c}}{f}$, the wave factor λ is calculated as $\lambda = \dfrac{2\pi}{\beta}$ and the phase shifting constant is denoted as β. Its value can be expressed as:

$$\beta = \omega\sqrt{\frac{\mu\varepsilon}{2}}\left(\sqrt{1+\left(\frac{\sigma}{\omega\varepsilon}\right)^2}\right)+1\,, \tag{5}$$

where ω is the angular frequency (rad/s), σ is conductivity in (S/m) and μ is permeability (H/m). The path loss due to attenuation in medium Θ_a is (in dB):

$$\Theta_a = 10\log \mathrm{e}^{-2\alpha d}\,, \tag{6}$$

where the attenuation constant is denoted by α. Its value can be calculated from:

$$\alpha = \omega\sqrt{\frac{\mu\varepsilon}{2}}\left(\sqrt{1+\left(\frac{\sigma}{\omega\varepsilon}\right)^2}\right)-1\,. \tag{7}$$

The parameters like propagation speed of EM waves v and the absorption coefficient ϑ are:

$$v \approx \frac{1}{\sqrt{(1+\chi_e)\times 8.85\times 10^{-12}\times\mu_r\times 4\pi\times 10^{-7}}}\,, \tag{8}$$

$$\vartheta = \frac{\sigma}{2}\times\sqrt{\frac{\mu_r\times 4\pi\times 10^{-7}}{(1+\chi_e)\times 8.85\times 10^{-12}}}\,, \tag{9}$$

where ε_0 and μ_0 are the permittivity and permeability of free space. The relative permittivity and permeability of sea water are denoted by ε_r and μ_r respectively.

5.2. Calculation of Reflection Loss of Water Boundaries

The reflection is caused by the boundaries of water bodies such as water-air and water-sand interfaces [18], as shown in Fig. 4. The value of the reflection coefficient, Γ can be expressed as:

$$\Gamma = \frac{\rho_2 v_2 - \rho_1 v_1}{\rho_2 v_2 + \rho_1 v_1}\,, \tag{10}$$

where the density of water is denoted as ρ_1 and of the other medium is signified as ρ_2. The wave velocity in water is denoted as v_1 and in another medium as v_2. The reflection

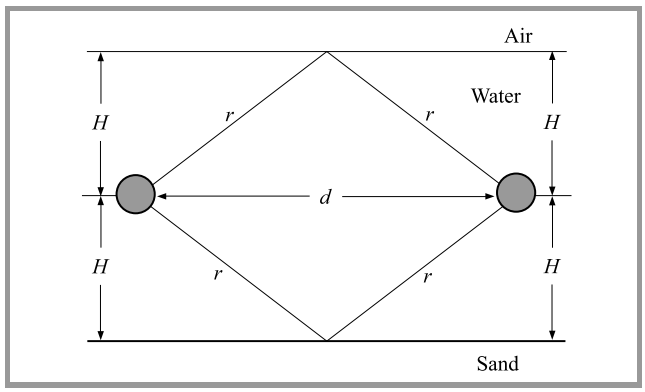

Fig. 4. Diagram representing the three-path reflection model.

loss from the surface and from the bottom is Θ_{ref} expressed as:

$$\Theta_{ref} = -V = -10\log V\,, \tag{11}$$

where V (in dB) is calculated as:

$$V^2 = 1 + \left(|\Gamma| e^{-\alpha\Delta(r)}\right)^2 - 2|\Gamma| e^{-\alpha\Delta(r)} \cos\left(\pi - \left(\phi - \frac{2\pi}{\lambda}\Delta(r)\right)\right), \tag{12}$$

where $\Delta(r)$ is the difference between r and d (in meters), $|\Gamma|$ and ϕ are the amplitude and phase of the reflection coefficient respectively and r is the reflected path length (in meters). The expression to calculate r is:

$$r = 2\sqrt{H^2 + \left(\frac{d}{2}\right)^2}\,. \tag{13}$$

5.3. Calculation of Throughput and Delay

The maximum throughput value is directly proportional to the payload bytes and inversely proportional to the delay experienced by each data packet [19]. The superframe structure of IEEE 802.15.4. is shown in Fig. 5. The precise

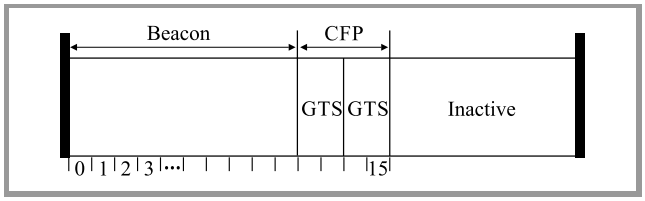

Fig. 5. Structure of the superframe in IEEE 802.15.4.

calculation of the delay and the determination of the number of payload bytes are very important to exactly calculate the maximum throughput. The total delay comprises of the

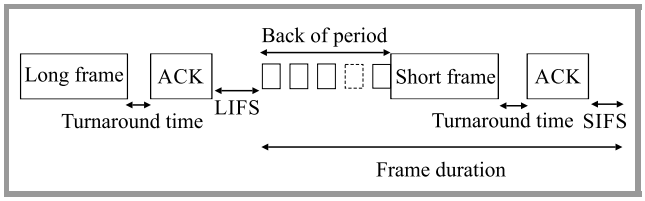

Fig. 6. The sequence of the IEEE 802.15.4 frames.

delay in data reception and the delay due to various frame sequences as shown in Fig. 6. Subsequently, the throughput ρ can be formulated as:

$$\rho = \frac{8 \cdot \varphi}{\delta(\varphi)}\,, \tag{14}$$

where φ denotes the payload bytes received from the network layer as shown in Fig. 7. The delay $\delta(\varphi)$ experienced by each packet can be expressed as:

$$\delta(\varphi) = \tau_{BO} + \tau_{frame}(\varphi) + \tau_{TA} + \tau_{ACK} + \tau_{IFS}(\varphi)\,, \tag{15}$$

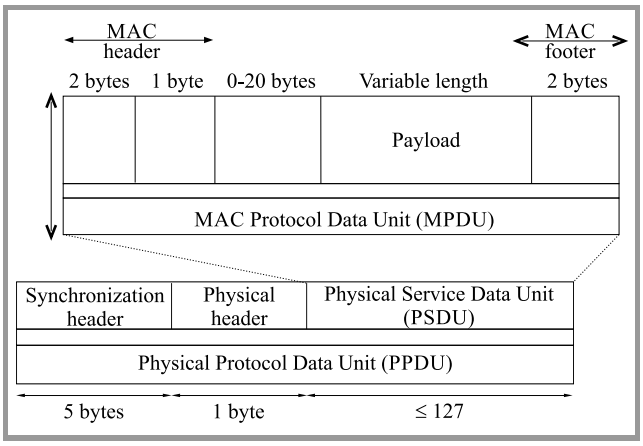

Fig. 7. Structure of the IEEE 802.15.4 frames.

where: τ_{BO} – back off period in s, $\tau_{frame}(\varphi)$ – transmission time for a payload of φ bytes in s, τ_{TA} – turnaround time in s, τ_{ACK} – transmission time for an ACK in s, $\tau_{IFS}(\varphi)$ – interframe sequence time in s, κ – payload size in bytes.

If the size of the MAC Protocol Data Unit (MPDU) is 18 bytes or less, then short interframe space (SIFS) is used for the interframe space (IFS). Otherwise, a long interframe space (LIFS) is used. The expression of the MAC Protocol Data Unit (λ) is given by:

$$\lambda = \phi + \mu + \kappa\,. \tag{16}$$

To calculate the total delay, it is important to calculate the time duration of its all components. The expression on the back off period is:

$$\tau_{BO} = \alpha \cdot \beta\,, \tag{17}$$

where α is the number of back off slots and β is the time for a back off slot.
The range of back off slots lies in the interval $(0,\, 2^{BE}-1)$, where BE means the *back off exponent* having a minimum value of 3. As, the communication channel is assumed as perfect the value of BE will remain the same. Therefore, the mean of the interval gives the number of back off slots which are: $\frac{2^{BE}-1}{1}$ or 3.5.
The total duration of the frame (in seconds) is:

$$\tau_{frame}(\varphi) = \frac{\psi + \phi + \Phi + \varphi + \mu}{\omega}\,, \tag{18}$$

where: ψ – length of the PHY header (6 bytes), ϕ – length of the MAC header (3 bytes), Φ – length of the information field of the MAC address (in bytes), μ – length of the MAC footer (2 bytes), ω – raw data rate (in b/s).

Equation (19) formulates the duration of an acknowledgement:

$$\tau_{ACK}(\varphi) = 8\frac{\psi + \phi + \mu}{\omega}\,. \tag{19}$$

The values of acknowledgement and turnaround times are 0, if acknowledgements are not used.

Finally, the throughput ρ (in b/s) and delay $\delta(\varphi)$ (in seconds) are expressed:

$$\rho \frac{8 \cdot \varphi}{m \cdot \varphi + n}, \tag{20}$$

$$\delta(\varphi) = m \cdot \varphi + n. \tag{21}$$

In the Eqs. (20)–(21), the values of m and n are influenced by the operating frequency of the channel, the length of data bytes in the payload (LISF or SIFS) and the length of the address. The values of parameters m and n are determined by using the curve fitting method considering the principle of least squares and by solving the respective normal equations to get the line of best fit.

5.4. Calculation of Jitter

To calculate jitter [20], let us assume the UWSN as a set M consists of n nodes, $M = \{M_1, M_2, M_3, \ldots, M_n\}$. Since each node periodically sends its status to the personal area network (PAN) coordinator or receives commands from it, we consider the set Γ' composed of n periodic tasks. Every task $\Gamma' j = (R_j, D_j, T_j) \in \Gamma'$ is characterized by the required number of timeslots R_j, a relative deadline D_j and the inter arrival time T_j. Effective tasks scheduling using adaptive active/sleep cycles is very important to reduce jitter. To avoid missing deadlines and to improve schedulability, the tasks are prioritized by various schedulers. When a task Γ'_j is scheduled at time slot s, the priority of this task P_j is calculated as:

$$P_j = D_j - s - T_j. \tag{22}$$

5.5. Calculation of Packets Dropped

In this paper, the Poisson process is implemented for the generation of packets at each sensor with parameter λ [21]. The exponentially distributed service time with parameter μ depends on the conduct of MAC protocols, and the influence of channel contention from other sensors. For the successful packet transmission, it should get completed within d time units after its arrival at the queue. For example, if a packet reaches at time t, it must get transmitted before its universal deadline $t + d$, where d is a fixed relative deadline. The probability of a successful packet transmission of the system is denoted as $PD(\theta)$ and its value is computed, where the packet dropping threshold, expressed in seconds, is denoted by θ. The number of packets present in the system, including the packets present in the transmitter immediately before a packet arrival is denoted by X. There are three states of the system experienced by a packet arriving in the system. These are empty, busy transmitter and full. The meaning of these states is explained as follows:

- *Empty* ($X = 0$) – the transmitter is available, and the buffer is empty as well;
- *Busy Transmitter* ($X = 1$) – the transmission of a packet is in progress but the buffer is empty;
- *Full* ($X = 2$) – the transmission is in progress and the buffer is full as well. In that case the reaching packet overwrites the packet already buffered.

The value of $PD(\theta)$ can be calculated depending on whether the packet arrives at an empty state or not. The service time experienced by the arriving packet is denoted by Q. The expression of $PD(\theta)$ is:

$$PD(\theta) = \Pi(X = 0)\,\Pi(Q \le d) + \\ + \big(1 - \Pi(X = 0)\big) \int_0^{d-\theta} \mu\, \mathrm{e}^{\mu t}\, \Pi(Q \le d - t)\, \mathrm{e}^{-\lambda t} \mathrm{d}t. \tag{23}$$

The transmission of an arbitrary packet Π, which arrives at an empty system, can be successful only if the required time Q is less than d. This explains the term $\Pi(X = 0)\Pi(Q \le d)$. If Π arrives when the system is busy in transmitting a packet ($X = 1$ or 2), the beginning of its transmission depends on the remaining transmission time t of the packet that is presently being transmitted. The density of the remaining service time is exponentially distributed as $\mu \mathrm{e}^{-\mu t}$. It is important to understand that these three conditions must be satisfied for the timely service of Π. First, the deadline duration is larger than θ when the remaining service ends, i.e. $d - t \ge \theta$. Second, it is explained by the factor $\Pi(Q \le d - t)$, which means that the service time is less than $t - d$. Third, the term $\mathrm{e}^{-\lambda t}$ explains it as there were no other arrivals during t time units. The representation of data packet arrivals and servicing is shown in Fig. 8.

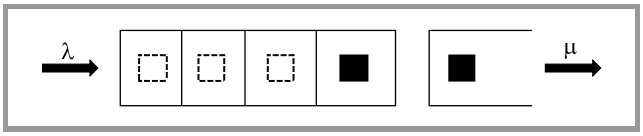

Fig. 8. The schematic representation of a queue.

5.6. Model of AR-MAC Protocol

Describing $f(t)$ as the transmitted signal sent from sensor node g to h, the expression of the transmitted signal is [22]:

$$f(t) = f(t + T_0), \tag{24}$$

where T_0 denotes the time duration of the signal. The received signal at sensor node h is defined as [22]:

$$z(t) = \mathrm{e}^{-j2\pi \frac{\varphi}{1+\varphi} f_c T_0} z\Big(t + \frac{T_0}{1+\varphi}\Big), \tag{25}$$

where φ is the Doppler scaling factor based on relative velocity between sensor nodes and the mobile sink, and the clock skew is denoted as δ. The summation of the signals that arrived along multiple physical paths is the received signal at the sink node and can be formulated as [22]:

$$Q_{hg}(t) = \sum_{k=1}^{N_k} A_k\, f_{gh}\big[(1 + \varphi_m)t - \tau_k)\big], \tag{26}$$

where $f_{gh}(t)$ is the message transmitted from sensor node g to h, with node g as the reference node. τ_k and A_k denote the delay and amplitude of the k-th path respectively. N_k signifies the number of paths. The joint Doppler scaling factor induced by the node mobility is thus $\varphi_m \cong \frac{v}{\sigma}$, where σ is the speed of electromagnetic waves in water and v is the relative velocity. The relative velocity of the two sensor nodes based on the joint Doppler scaling factor φ_m can be directly obtained from [22]:

$$v \cong \varphi_m \sigma = \big((1+\varphi_{gh})\phi - 1\big)\sigma\,, \tag{27}$$

the ϕ signifies clock skew and φ_{gh} is Doppler scaling factor for sensors g and h. Finally, the propagation delay is [22]:

$$\tau = \frac{\delta\sigma - \phi t_r(\sigma + \vartheta) - \mu}{2\phi\sigma}\,, \tag{28}$$

where ϑ is the velocity of the mobile sink (in m/s), $t_r = t_3 - t_2$ and $\delta = t_4 - t_1$ as t_1, t_2, t_3 and t_4 are different time instants, $\mu = \frac{1}{2\alpha t_r^2}$ as α denotes acceleration of the mobile sink node.

Let v be the velocity of the mobile sink. D_{ij} is the path length in meters from location i to j during, which the sensor nodes from S_i to S_j are active and is expressed as:

$$D_{ij} = v(\tau_j - \tau_i)\ \forall i, j\,. \tag{29}$$

The sensors are having different on/off time periods depending on the location and velocity of the mobile sink. The sensor number S_i active during the i-th time slot τ_i is expressed as:

$$\sum_{i}^{i+3} S_i = \tau_i, \quad \text{where} \quad i = 1\,, \tag{30}$$

$$\sum_{j}^{j+3} S_j = \tau_j, \quad \text{where} \quad j = i+3\,. \tag{31}$$

The expression for the n-th number of sensor is:

$$\sum_{n}^{n+3} S_n = \tau_n, \quad \text{where} \quad n = j+3\,. \tag{32}$$

The total simulation time T_{sim} is 670 s for 100 nodes and 1395 s for the 200 nodes:

$$T_{sim} = \overset{\tau_1}{\underset{0}{T_1}} + \overset{t_2}{\underset{\tau_1+1}{T_2}} + \ldots + \overset{t_n}{\underset{\tau_{n-1}}{T_n}}\,. \tag{33}$$

The duty cycle of each sensor node (RFD) is adjusted by varying the on/off time. In the proposed scenario a sensor node is active for 28 s, which means that for a 100 node network, with the total simulation time of 670 s, the duty cycle is about 4.1%.

Likewise, for a network of 200 nodes, having the total simulation time of 1395 s, the duty cycle is about 2%. The aim of the proposed AR-MAC is to minimize the average end-to-end delay, minimize jitter, and to improve other performance metrics. The aim to achieve a minimum average end-to-end delay is:

$$Aim = \min \delta(\varphi)\,. \tag{34}$$

5.7. Analysis of the Proposed Queuing Model

The proposed queueing model uses the slotted CSMA-CA channel access mechanism in a beaconed mode of operation. In order to transmit data, the device needs a guaranteed time slot during the contention-free period (CPF). If the channel is busy, during the contention access period the device waits for a random number of unit back-off periods ($\sum$) with the range of (0, $2^{BE}-1$) before performing the clear channel assessment (λ). The transmission takes place if the channel is at idle. Otherwise it has to wait for another random period before trying to access the channel again. The initial value of the back off exponent *BE* is equal to *macMinBE*.

Assuming that the channel is free and that the default *macMinBE* value is 3, the worst-case channel access time can be calculated as:

$$\int_{CSMA\text{-}CA} = \varsigma + \lambda \Rightarrow (2^3 - 1)\sum + \lambda \Rightarrow 2.368 \text{ ms}\,. \tag{35}$$

The duration of one symbol period is 16 μs, *aUnitBackoffPeriod* is equal to 20 symbol periods and the clear channel assessment detection time is equal to the duration of 8 symbol periods. The data frame transfer time denoted as $\int_{Data}$ of a channel having the data rate of (C) 250 kb/s is expressed in Eq. (36), where $\wp$ is the *MaxPHYPacketSize*.

$$\int_{Data} = \frac{\wp 8}{C}\,, \tag{36}$$

$$\int_{Data} = 4.064 \text{ ms}\,.$$

The size of an acknowledgement frame is 11 bytes. At the fundamental data rate of 250 kb/s, its transmission takes 0.352 ms. The transmission of acknowledgement uses the CSMA-CA mechanism. The transmission of an acknowledgement frame commences *aTurnaroundTime* symbols after the reception of the data frame, where *aTurnaroundTime* is 192 μs. This allows the device enough time to switch between transmitting and receiving modes. The maximum data payload is 127 bytes. The expression for effective service time using a stop-and-wait Automatic Repeat Request (ARQ) protocol can be calculated as:

$$\int_0 = \int_{CSMA\text{-}CA} + \int_{Data} + \int_{Turnaround} + \int_{Ack} + \int_{Prop}\,, \tag{37}$$

where $\int_{Prop}$ is the propagation time between the sensor node and the sink. The value of $\int_{Prop}$ is negligible and can be ignored in the calculation, and $\int_{Ack}$ is the acknowledgement transmission time.

In this model, the sensors relay the sensed data directly to the sink node using single hop. The transmission time through the single-hop can be calculated as:

$$\int_{s\_hop} = \int_{single\_hop} + \Delta\,, \tag{38}$$

where $\int_{single\_hop}$ is the transmission time taken to transmit one data frame through one hop. In this case, $\int_{single\_hop} = \int_0$, Δ is the processing time for routing.

The overall packet loss rate denoted as $\Re_{Totalloss}$, may constitutes of packet loss due to dropping from the queue with the rate of overflow ($Re_{Overflow}$), or due to channel errors. The packet error rate at physical layer is denoted as $\Re_{Phy}$. The rate of packet loss over the wireless channel, after U times of packet retransmissions, will be:

$$\Re_{Phyloss} = \Re_{Phy}^{U+1}. \tag{39}$$

Consequently, the overall packet loss rate will be:

$$\Re_{Totalloss} = \Re_{Overflow} + (1 - R_{Overflow})\Re_{Phyloss}. \tag{40}$$

Neglecting the value of $R_{Overflow} \times \Re_{Phyloss}$ as it is negligible; the total packet loss rate can be approximated as:

$$\Re_{Totalloss} = \Re_{Overflow} + R_{Phyloss}. \tag{41}$$

In this paper, the M/M/1 queuing model with the Poisson distribution arrival rate λ and the exponential service time μ is implemented. The probability density function (PDF) denoted as $g(t)$ of service time is:

$$g(t) = \mu e^{-\mu t}. \tag{42}$$

In the retransmission model, the PDF of the service time due to the packet transmission can be calculated as:

$$g(t) = \sum_{w=0}^{U} g\left(\frac{t}{w}\right) P(w), \tag{43}$$

where the probability of attempting w retransmissions of a single packet to succeed or to reach the retry-limit U is denoted as $P(w)$ and $g(\frac{t}{w})$ denotes the service time conditional PDF, given w retransmissions of a single packet. The $P(w)$ is:

$$P(w) = (1 - \Re_{Phy})\,\Re_{phy}^{w}. \tag{44}$$

The service time at the w-th retransmission is formulated as:

$$\mu = \mu_0 (w+1), \tag{45}$$

where μ_0 is the service time of system without an error in the wireless channel. The μ is 6.976 ms.

So, the service time conditional PDF, given that w retransmissions of a single packet, is:

$$g\left(\frac{t}{w}\right) = \mu\, e^{-\mu_w t} \tag{46}$$

from Eqs. (42)–(45), the service time due to the packet retransmission can be written as:

$$g(t) = \mu_0 e^{-\mu_0 t} + \mu_0 \sum_{w=1}^{U} \Re_{Phy}^{w} \left(\frac{1}{w+1} e^{\frac{-u_0}{w+1} t} - \frac{1}{w} e^{\frac{-\mu_0}{w} t} \right). \tag{47}$$

The mean value for service time $E\big(g(t)\big)$ is defined as:

$$E\big(g(t)\big) = \mu = \mu_0 \frac{1 - \Re_{Phy}}{1 - \Re_{Phy}^{U+1}}. \tag{48}$$

In this model every sensor node has a finite queue length denoted as Q. Therefore, the packet overflow drop rate is equal to the probability that a packet cannot find available room for storage, and is hence dropped.
With one packet under service, the overflow rate can be formulated as:

$$\Re_{Overflow} = \sum_{i=Q+1}^{\infty} (1-\rho)\rho^{i} = \rho^{Q+1}. \tag{49}$$

The total packet loss for the M/M/1 queuing model can be written as:

$$\Re_{Totalloss} = \left(\frac{\lambda_0}{\mu_0} \frac{1 - \Re_{Phy}^{U+1}}{1 - \Re_{Phy}} \right)^{Q+1} + \Re_{Phy}^{U+1}. \tag{50}$$

The average number of packets in the system is:

$$\overline{\Im} = \frac{\rho}{1-\rho} = \frac{\lambda}{\mu - \lambda}. \tag{51}$$

The average time spent in the system is:

$$\Delta = \frac{\overline{\Im}}{\lambda} \frac{\rho}{1-\rho} \frac{1}{\lambda} = \frac{1}{\mu - \lambda}, \tag{52}$$

where $\rho = \frac{\lambda}{\mu}$. The average spending time will be:

$$\Delta = \frac{1}{\mu_0 \cdot \dfrac{1 - P_{phy}}{1 - P_{Phy}^{U+1}} - \lambda}. \tag{53}$$

6. Simulation Scenario and Algorithms

Figure 9 shows the general scenario of UWSNs consisting of different types of sensor nodes and autonomous underwater vehicles used for collaborative monitoring. The

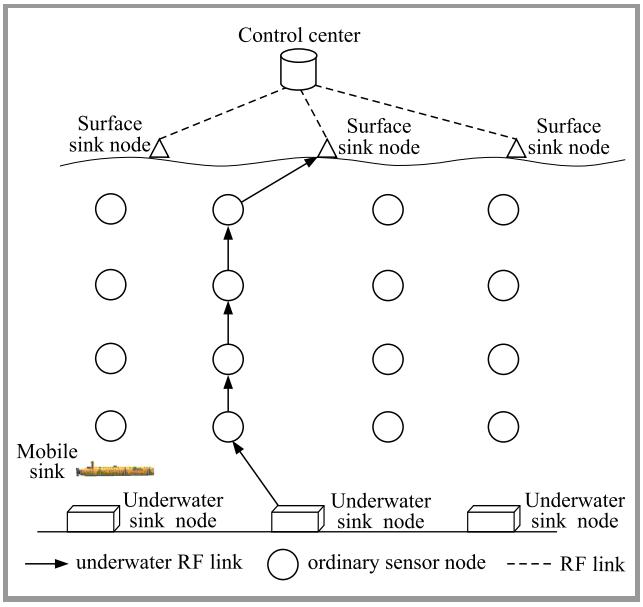

Fig. 9. General scenario of UWSN.

underwater sensors are linked with each other via microwave links. Further, the surface sink nodes are connected to the control center via RF links. The architectures are application dependent, either of the 3D or 2D variety. The ordinary sensor nodes sense and relay data using a direct link, or through a multi-hop path. The mobility of sensor nodes, as well as of sink nodes can be classified as controlled mobility and uncontrolled mobility. This paper implements radio links for both underwater and free space communication. The sensed data are transmitted through direct radio links and the mobility of the sink node is controlled.

The lawn mower trajectory of the mobile sink, as shown in Fig. 10, is considered after extensive simulations to reduce the requirement of multi-hop data transmissions. The network constitutes of RFDs, except for the mobile sink, to avoid multi-hop data transmissions and to reduce the depletion of battery power. This trajectory is most suitable, as the sink node is available for all sensors within their transmission range after the regular interval of times, but at the cost of an increased path length. The deteriorating effect of the increased path length is reduced by implementing an effective path determination (EPD) algorithm. The velocity of the sink node is selected so that each sensor node gets sufficient time to synchronize and to transmit the sensed data without the requirement of any sojourns.

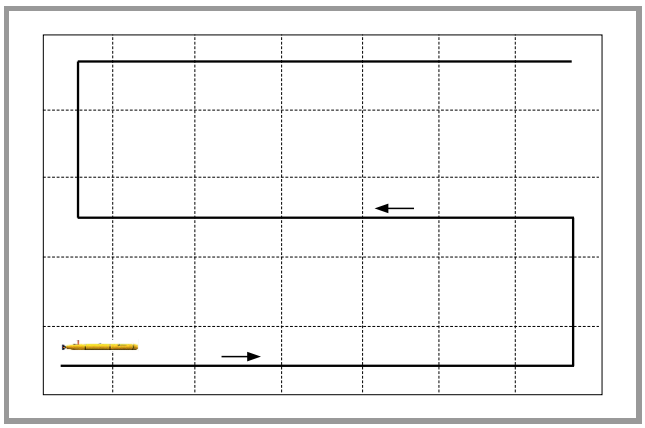

Fig. 10. Representation of the mobile sink's Lawn-mower trajectory.

The expression of transmission data rate r of data sent to sensor q denoted by r_q [23] can be written as:

$$r_q = B\log_2\left(1+\frac{p_q g_q(x^*,y^*)}{\sum_{m=q+1}^{n} P_m h_q(x^*,y^*)+N_0}\right) = l_q K_r^*, \quad (54)$$

where B is the available bandwidth, P_q is the power assigned to transmission to sensor q, $g_q(x^*,y^*)$ is the channel gain as a function of the distance, K_r^* is the ratio of rate of transmissions to the message length, l_q is the length of the message sent to sensor q, and N_0 is the expected ambient noise. To attain the transmission power P_i in the terms of x^*, y^* and K_r^*, Eq. (54) can be recursively solved to:

$$P_i(x^*,y^*,k_r^*) = (2^{L_q K_r^*}-1)\frac{N_0+\sum_{m=q+1}^{n} P_m(x^*,y^*,K_r^*)h_q(x^*,y^*)}{h_q(x^*,y^*)}. \quad (55)$$

Equation (55) illustrates the influence of all prime parameters on the power allotted to the transmission to sensor i. To determine the effective path length and the optimum throughput path, the sink needs to evaluate the maximum K_r possible over the entire network and then select the position with the highest K_r.

Algorithm 1 is proposed to find out the effective path length and Algorithm 2 to determine the maximum throughput path for the mobile sink. It is assumed that the sensors are properly anchored to limit their movement due to waves within the permissible limits to follow these algorithms.

The network scenario presented in this paper has implemented different queue types as FIFO, random early detection (RED), random early detection with I/O bit and weighted random early detection. Each of them is implemented with different queue sizes in bytes such as 20,000, 22,000, 25,000, 26,000, 27,000, 30,000, 50,000, 150,000, 200,000, 250,000, 500,000 and 1,000,000. The schedulers employed are differentiated as services weighted fair, round robin and self-clocked fair. The intent is to effectively schedule the transmission and reception of data packets.

Algorithm 1: Effective path length determination

State 1: The initial position of the mobile sink.
The initial position be P on the water surface.
Let the desired position is $\mathscr{P}$.
while $P \neq \mathscr{P}$ **do**
  $P = \mathscr{P}$
  State 2: Connections using radio channel
  Initialize the maximum range $= r_{\max}$.
  The location of the sensor k is L_k.
  The total number of sensors in the network is N.
  The point of the present position of the sensor k is L_k^m while sink and sensor node k distance is $D_{k,m}$.
  $D_{k,m} = \| L_k^m - P \|, \forall L_k^m \in P$.
  if $D_{k,m} \leq r_{\max}$ **then**
    Path found; break.
  end if
  State 3: Revaluate effective path and reallocate sensors
  Find P that minimizes max $\| L_k^m - P \| \, \forall P \in L_k^m$.
  if $P = \mathscr{P}$ and $D_{k,m} > r_{\max}$ for any m **then**
    No path found; break
  end if
end while
State 4: Location modification
Solve the Eq. (55) to attain the optimal location to achieve the maximum K_r for the sink node.

Algorithm 2: Optimum throughput path determination

Initialize: number of segments $S = 1$;
iteration time $q = N$, set segment $(k) = 1 \forall\, k$
Generate $n \times n$ distance matrix X and calculate throughput $\hbar$.
while $q > 0$ **do**
  Find the reference throughput $\hbar$ at distance $r_{\max} =$ 20 m.
  if $\hbar_{new} \geq \hbar$ **then**
    Optimum throughput path found. Delete entries in X corresponding to k.
    $S = S + 1; \quad q = q + 1$
  end if
end while
State: Recalculate optimum throughput path
while $q > 0$ **do**
  if $\hbar_{new} < \hbar$ **then**
    Optimum throughput path not found.
  end if
end while
Solve the Eq. (55) to attain the optimal location to achieve the maximum K_r for the sink node.

7. Simulations Results and Analysis

The simulation parameters are shown in Table 1. The simulations are performed using the Qualnet 6.1 software. Ten simulation rounds are performed and their average value is considered to obtain more accurate results. The flowchart demonstrating steps followed in the simulation process is shown in Fig. 11.

Table 1
Simulation parameters

No.	Parameter	Value
1	Total number on nodes	101, 201
2	Number of PAN coordinators	1, 1
3	Number of RFDs	100, 200
4	Communication protocols	
	RFDs to PAN coordinator	IEEE 802.15.4
	PAN to RFDs	IEEE 802.15.4
5	Operating frequency	2.4 [GHz]
6	Packet size	38 [bytes]
7	Packet interval	1 [s]
8	Simulation times	670, 1395 [s]
9	Battery	1200 [mAh]
10	Transmission range	20 [m]
11	Node connectivity	Protocol, frequency [GHz]
	RFDs to PAN	ZigBee, 2.4
	PAN to RFDs	ZigBee, 2.4
12	Terrain area	$110 \times 20 \times 110$ m $210 \times 20 \times 110$ m
13	Energy model	Mica-motes
14	Battery model	Linear
15	Optimum queue size	26,000 [bytes]
16	Queue type	FIFO
17	Scheduler type	DSWF
18	Application	Traffic generator
19	Speed of PAN	0.7164 [m/s]

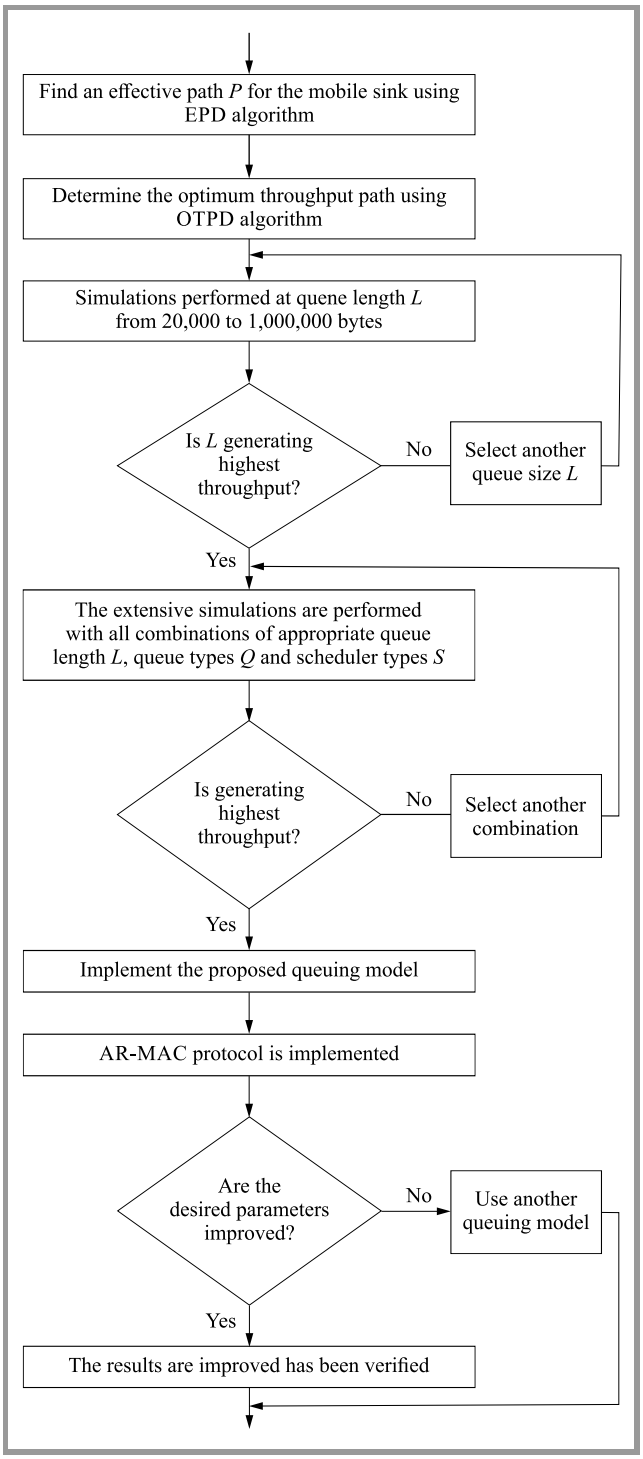

Fig. 11. Flowchart of the proposed model.

To validate the influence of queue size, queue type and scheduler type, performance parameter is calculated first to find out the most suitable queue size, as shown in Fig. 12, and to find out the most appropriate combination of types of queues and schedulers with the most efficient queue size, as

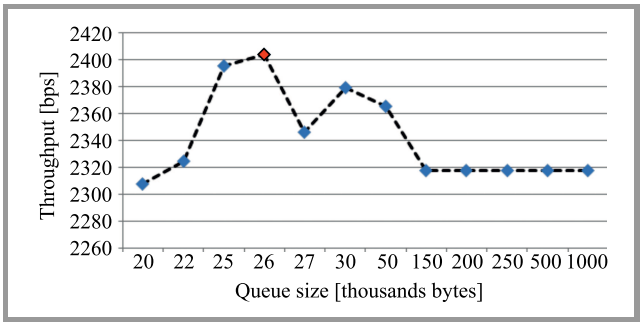

Fig. 12. Performance evaluation at different queue sizes.

shown in Fig. 13. The throughput at different queue lengths shown in Fig. 12 and the throughput for various combinations of queue types and scheduler types at the queue length of 26,000 bytes is considered as the performance parameter. It is observed that the maximum throughput is achieved at the queue size of 26,000 bytes, using a round robin scheduler with a random early detection queue. A more precise analysis of individual parameters, such as packets de-queued, packets dropped, packets queued, average queue length, longest time in queue, peak queue length, average time in queue and total number of packets dropped, is still required to finalize the selection of most the suitable queue and scheduler types.

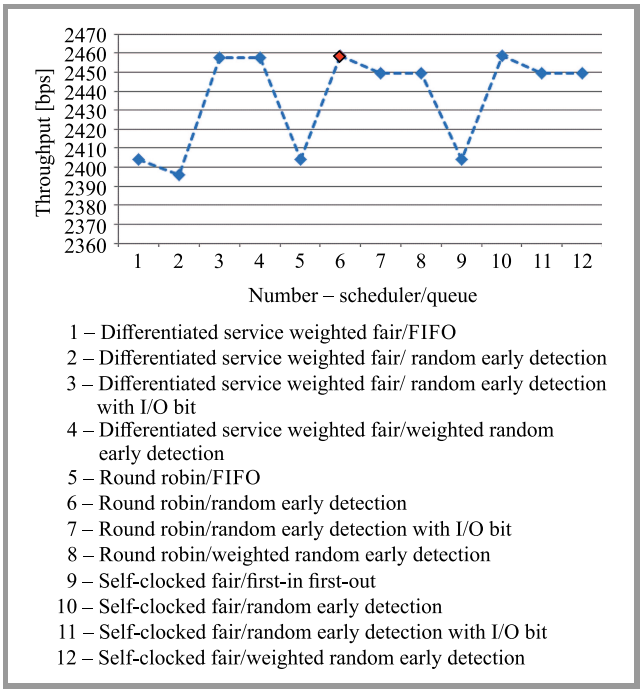

Fig. 13. Performance evaluation using different schedulers and queues of 26,000 bytes.

An extensive analysis of results, presented in Figs. 14 to 20, indicates that differentiated service-weighted fair schedulers, paired with the FIFO queue, at the queue size of 26,000 bytes, are chosen for the final simulation.

The number of packets de-queued at different queue sizes is presented in Fig. 14. The number of de-queued packets is the lowest at the queue size of 20,000 bytes. With the further increase in queue size it also decreases at the size of 26,000 bytes. Finally, above the queue size of 200,000 bytes, it becomes stable at the same value that is achieved at the size of 26,000 bytes.

The number of packets dropped at different queue sizes is shown in Fig. 15. It can be seen that at a low queue size the number of packets dropped is higher and decreases with the increase in queue size. At the size of 500,000 and 1,000,000 bytes, its value becomes almost negligible.

Fig. 14. Number of packets de-queued.

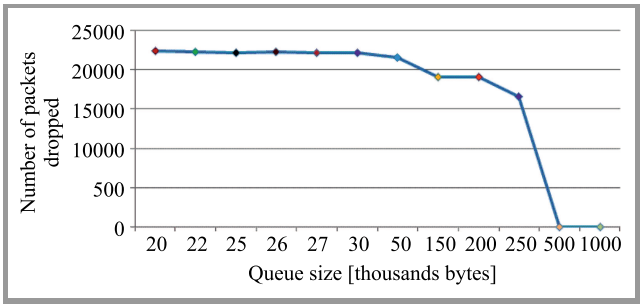

Fig. 15. Number of packets dropped.

The number of packets queued is directly proportional to the queue size (Fig. 16). With an increase in queue size, the capacity to queue the data packets also increases, which prevents the packets from being dropped.

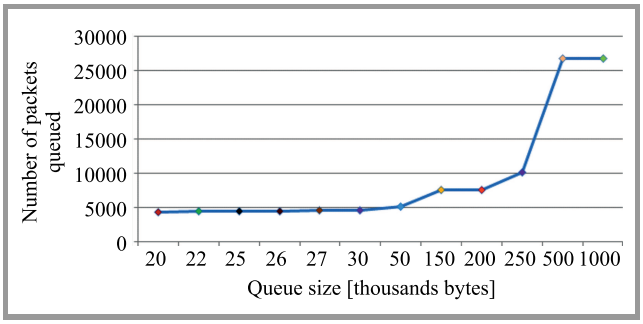

Fig. 16. Number of packets queued.

The average queue length for different combinations of different types of queues and schedulers at the queue size of 26,000 bytes is shown in Fig. 17. It is largest for the FIFO and smallest for the RED queue.

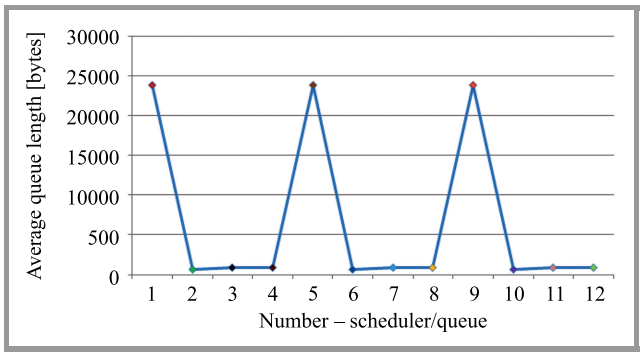

Fig. 17. The average queue length. The *x* axis legend is from Fig. 13.

The longest time spent by the data packets in the queues is presented in Fig. 18. The longest time taken is in the FIFO queue, and the shortest time is in the RED queue.

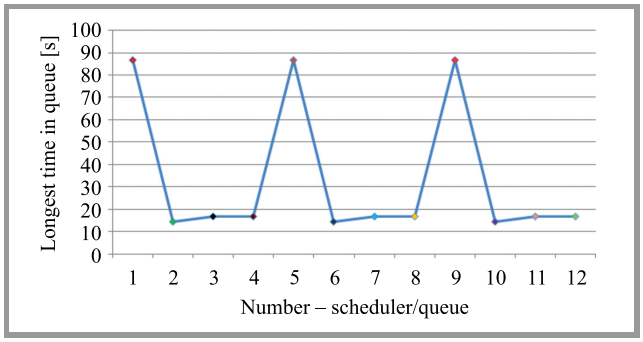

Fig. 18. The longest time in queue. The *x* axis legend is from Fig. 13.

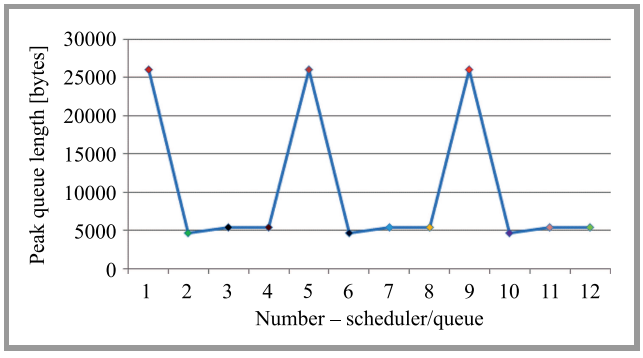

Fig. 19. The peak queue length – see legend box in Fig. 13.

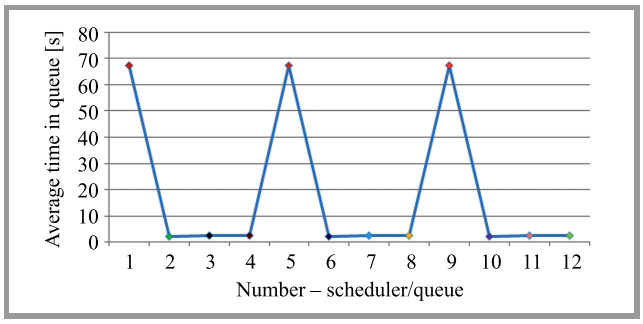

Fig. 20. The average time in queue – see legend box in Fig. 13.

The peak queue length is evaluated and compared in Fig. 19. The highest value is for the FIFO, which gets reduced for WRED, reduced even further for the RIO, and the minimum value is achieved for the RED queue.
The average time in the queue is evaluated and presented in Fig. 20. The longest time in the queue is for the FIFO, and the shortest time is for the RED queue.

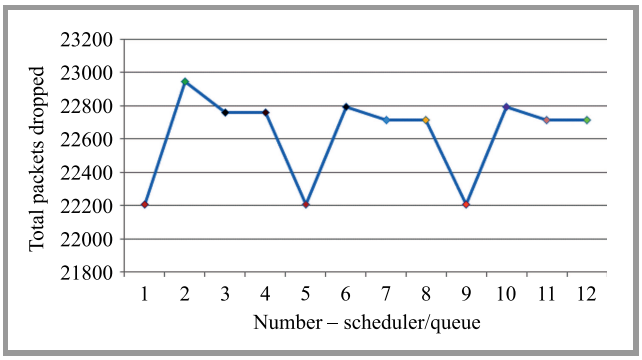

Fig. 21. The number of total packets dropped – to decipher *x* axis values, see legend box in Fig. 13.

The number of total packets dropped in the combination of different queues and schedulers is analyzed in Fig. 21. The results show that the combination of different schedulers with the FIFO queue has the lowest number of packets dropped, equaling to 22,200 packets.

8. The Comparison of IEEE 802.15.4 and AR-MAC

The evaluation and analysis of different parameters, such as packets queued, packets de-queued, average queue length, longest time in a queue, peak queue length and average time in a queue, results in the determination of the most appropriate combination. Implementation of the Differentiated Service Weighted Fair scheduler with the FIFO queue at the queue size of 26,000 bytes is considered for the simulations with the proposed queuing model and the AR-MAC protocol.
Evaluation and comparison of the total number of packets dropped for IEEE 802.15.4 and AR-MAC protocol is shown

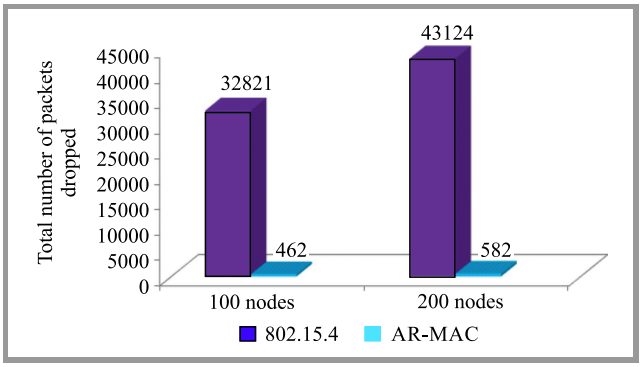

Fig. 22. The comparison of total number of packets dropped.

in Fig. 22. The result shows a significant reduction in the packets dropped when using the AR-MAC protocol in the networks of 100 and 200 nodes.

The average queue length is calculated and compared in Fig. 23. Utilization of the AR-MAC protocol significantly reduces the average queue length for the networks of 100 and 200 nodes. It will decrease the end-to-end delay, as the waiting time of the data packets is significantly reduced.

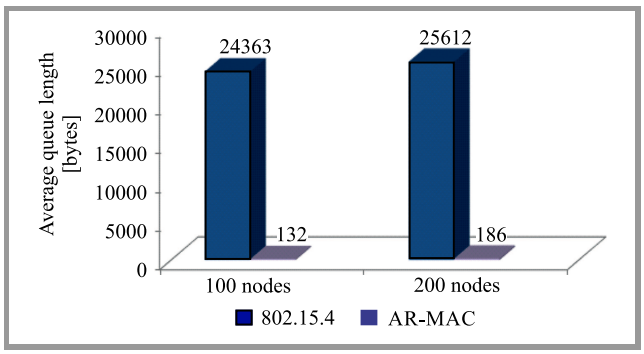

Fig. 23. The comparison of average queue length.

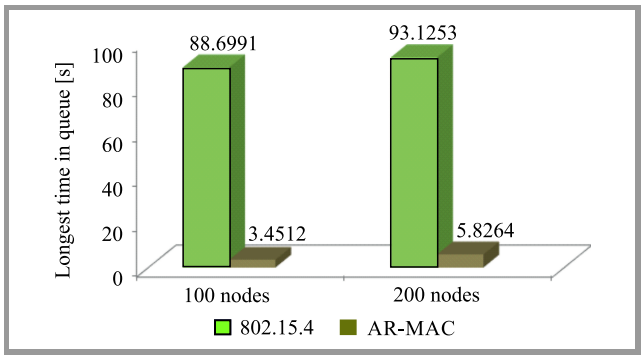

Fig. 24. The comparison of longest time in queue.

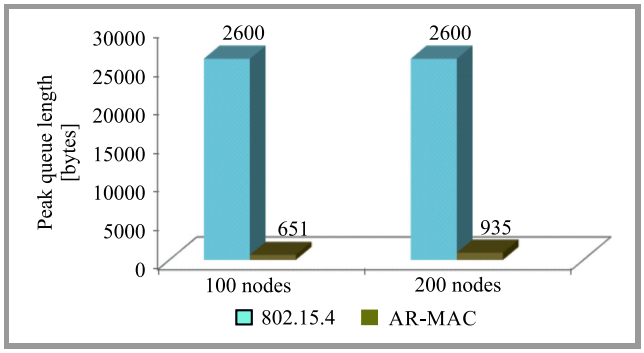

Fig. 25. The comparison of peak queue length.

The longest time in the queue is evaluated and compared in Fig. 24. The performance of AR-MAC is still better than that of the IEEE 802.15.4 protocol for the networks of 100 and 200 nodes.

The peak queue length for IEEE 802.15.4 and AR-MAC for the networks of 100 and 200 nodes is compared in Fig. 25. It is negligible for the AR-MAC protocol.

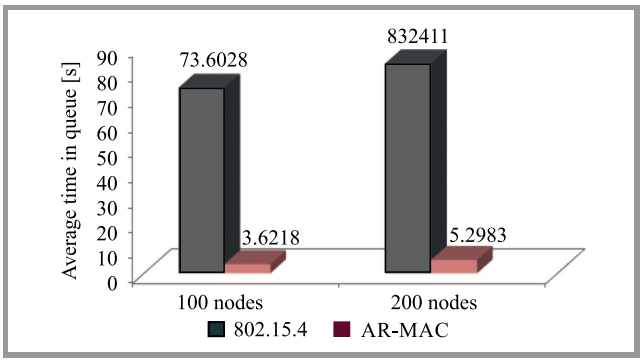

Fig. 26. The comparison of average time in queue.

The average time in the queue, which contributes to the end-to-end delay, is negligible for the AR-MAC protocol, as shown in Fig. 26. It has been verified that the AR-MAC protocol is appropriate to optimize the performance of schedulers and queues in the sink and sensor nodes.

9. Conclusion and Future Work

In this paper, we have implemented the AR-MAC protocol with effective path and optimum throughput path determination algorithms after the determination of queue size, queue type and scheduler type. The aim of optimizing the performance of queues has been successfully achieved along with the improvement in other performance metrics. Simulation results validate the proposed protocol under various application requirements and network conditions. Implementation of efficient scheduling algorithms to enhance the output of the network layer, which leads to optimized performance of the MAC layer, is a very effective technique. The aim is to prevent the overflow of queues – resulting in congestion and formation of bottlenecks – to eliminate the loss of data packets carrying important information.

In the future, we intend to develop a queuing model for the static sink UWSNs.

References

[1] I. F. Akyildiz, D. Pompili, and T. Melodia, "Underwater acoustic sensor networks: research challenges", *Ad Hoc Networks*, vol. 3, no. 3, pp. 257–279, 2005.

[2] I. F. Akyildiz, D. Pompili, and T. Melodia, "State of the art in protocol research in underwater acoustic sensor networks", *ACM Mob. Comput. Commun. Rev.*, vol. 11, no. 4, pp. 11–22, 2007.

[3] L. Weifa, L. Jun, and X. Xu, "Prolonging network lifetime via a controlled mobile sink in wireless sensor networks", in *Proc. of IEEE Global Telecommun. Conf. GLOBECOM 2010*, Miami, FL, USA, 2010 (doi: 10.1109/GLOCOM.2010.5683095).

[4] J. K. Jalaja and J. Lillykutty, "Delay and lifetime performance of underwater wireless sensor networks with mobile element based data collection", *Int. J. of Distrib. Sensor Netw.*, vol. 8, no. 1, pp. 1–22, 2015.

[5] S. Sendra, J. Lloret, J. J. P. C. Rodrigues, and J. M. Aguiar, "Underwater wireless communications in freshwater at 2.4 GHz", *IEEE Commun. Lett.*, vol. 17, no. 9, pp. 1794–1797, 2013.

[6] E. Ali, E. Abdelrahman, A. Majed, and E. Khaled, "Underwater wireless sensor network communication using electromagnetic waves at resonance frequency 2.4 GHz", in *Proc. of of the ACM 15th Commun. and Netw. Simulation Symp. CNS'12*, Orlando, FL, USA, 2012.

[7] B. Latré, P. De Mil, I. Moerman, B. Dhoedt, and P. Demeester, "Throughput and delay analysis of unslotted IEEE 802.15.4", *J. of Networks*, vol. 1, no. 1, pp. 20–28, 2006.

[8] K. Yu, M. Gidlind, J. Akerberg, and M. Bjorkman, "Low jitter scheduling for industrial wireless sensor and actuator networks", in *Proc. of the 39th Ann. Conf. of the IEEE Industrial Electron. Soc. IECON 2013*, Vienna, Austria, 2013, pp. 5594–5599.

[9] M. Aoun and A. Argyriou, "Queueing model and optimization of packet dropping in real-time wireless sensor networks", in *Proc. of the IEEE Global Commun. Conf. GLOBECOM 2012 – Commun. QoS, Reliab. and Model. Symp.*, Anaheim, CA, USA, 2012, pp. 1687–1691.

[10] J. Liu *et al.*, "DA-Sync: A Doppler-Assisted time synchronization scheme for mobile underwater sensor networks", *IEEE Trans. on Mob. Comput.*, vol. 13, no. 3, pp. 582–595, 2014.

[11] H. Yang and B. Sikdar, "A mobility based architecture for underwater acoustic sensor networks", in *Proc. IEEE Global Telecommun. Conf. GLOBECOM 2008*, New Orleans, LA, USA, 2008.

[12] N. Tuan Le, S. Woong Choi, and Y. Min Jang, "Approximate queuing analysis for IEEE 802.15.4 sensor network", in *Proc. 2nd Int. Conf. on Ubiquit. and Future Netw. ICUFN 2010*, Jeju Island, Korea (South), 2010, pp. 193–198.

[13] S. Charalambos, V. Vasos, and P. Aristodemos, "Estimating queue formation rate in Wireless Sensor Networks using a fluid dynamic model", in *Proc. 20th IEEE Symp. on Comp. and Commun. ISCC 2015*, Larnaca, Cyprus, 2015, pp. 544–548.

[14] N. Van Mao and V. Que Son, "Applying queuing theory to evaluate performance of cluster wireless sensor networks", in *Proc. Int. Conf. on Adv. Technol. for Commun. ATC 2015*, Ho Chi Minh City, Vietnam, 2015.

[15] J.-F. Ke, W.-J. Chen, and D.-C. Huang, "Life extend approach based on priority Queue N strategy for wireless sensor network", in *Proc. 11th In. Conf. on Heterogen. Netw. for Qual., Reliabil., Secur. and Robustness QSHINE 2015*, Taipei, Taiwan, 2015.

[16] S. Vanithamani and N. Mahendran, "Performance analysis of queue based scheduling schemes in wireless sensor networks", in *Int. Conf. on Electron. and Commun. Syst. ICECS 2014*, Coimbatore, India, 2014.

[17] H. Byun and J. Yu, "Adaptive duty cycle control with queue management in wireless sensor networks", *IEEE Trans. on Mob. Comput.*, vol. 12, no. 6, pp. 1214–1224, 2013.

[18] E. G. W. Peters, D. E. Quevedo, and M. Fu, "Controller and scheduler codesign for feedback control over IEEE 802.15.4 networks", *IEEE Trans. on Control Syst. Technol.*, vol. 1, no. 99, pp. 2459–2464, 2016.

[19] B. Pati, J. L. Sarkar, C. R. Panigrahi, and R. K. Verma, "CQS: A Conflict-free query scheduling approach in wireless sensor networks", in *Proc. 3rd Int. Conf. on Recent Adv. in Inform. Technol. RAIT 2016*, Dhanbad, India, 2016, pp. 13–18.

[20] H. Zhang *et al.*, "Scheduling with predictable link reliability for wireless networked control", in *Proc. 23rd Int. Symp. on Quality of Service IWQoS 2015*, Portland, OR, USA, 2015.

[21] B. Pati, J. L. Sarkar, C. R. Panigrahi, and M. Tiwary, "ARTQS: An advanced real-time query scheduling approach in wireless sensor networks", in *Proc. Int. Conf. on Green Comput. and Internet of Things ICGCIoT 2015*, Delhi, India, 2015, pp. 219–224.

[22] E. G. W. Peters, D. E. Quevedo, and M. Fu, "Co-design for control and scheduling over wireless industrial control networks", in *Proc. 54th IEEE Conf. on Decision and Control CDC 2015*, Osaka, Japan, 2015, pp. 2016–2030.

[23] M. H. Shahid and Sh. Masud, "Improved low power scheduler for OSS-7: An open source DASH7 stack", in *Proc. IEEE Int. Conf. on Electron., Circuits, and Syst. ICECS 2015*, Cairo, Egypt, 2015, pp. 645–648.

[24] M. Chovanec and P. Sarafin, "Real-time schedule for mobile robotics and WSN applications", in *Proc. Federated Conf. on Comp. Sci. and Inform. Syst. FedCSIS 2015*, Lodz, Poland, pp. 1199–1202.

[25] M. A. Jamshed *et al.*, "An energy efficient priority based wireless multimedia sensor node dynamic scheduler", in *Proc. 12th Int. Conf. on High-capacity Opt. Netw. and Enabling/Emerging Technol. HONET 2015*, Islamabad, Pakistan, 2015, pp. 147–150.

Vikas Raina completed his B.E. in Electronics and Communication Engineering and M.Tech. in microelectronics and VLSI Design from Rajiv Gandhi Technical University, Bhopal, India. He is pursuing his Ph.D. in Underwater Wireless Sensor Networks from Mody University of Science and Technology, Lakshmangarh, Rajasthan. Mr. Vikas Raina has more than 11 publications in national and international journals and conferences.
E-mail: vikasraina.cet@modyuniversity.ac.in
Department of ECE, CET
Mody University of Science and Technology
Lakshmangarh, India

Manish Kumar Jha completed his B.E. in Electronics Engineering from Bangalore University and Ph.D. from Birla Institute of Technology, Mesra, Ranchi. He has more than 23 years of extensive experience in teaching and industry out of which he has spent more than 11 years as an academic with Birla Institute of Technology, Mesra Ranchi. Presently he is the Director of ABES Engineering College, Ghaziabad, India. Before joining ABES EC, he was working at Mody University of Science and Technology, Lakshmangarh, as Professor and Associate Dean. He is a very able administrator and a learned scholar. One Ph.D. has been awarded and several scholars are pursuing doctoral research under his guidance. He has guided more than 20 M.Tech. projects. Prof. Manish Kumar Jha has played many other roles over two decades of his career. A project concerned with design and simulation of a new energy efficient ML-MAC wireless sensor protocol, funded by ISRO, was successfully completed under his leadership and guidance. Prof. Manish Kumar Jha has more than 40 publications in national and international journals and conferences.
E-mail: manishkjhaa@gmail.com
ABES Engineering College
Ghaziabad, India

Partha Pratim Bhattacharya has 20 years of experience in teaching and research. He served many reputed educational institutes in India in various positions. At present, he is working as Professor in the Department of Electronics and Communication Engineering in the College of Engineering and Technology, Mody University of Science and Technology (formerly, Mody Institute of Technology and Science), Rajasthan, India. He has published more than 100 papers in reputed journals and conferences. His present research interests include mobile cellular communication, wireless sensor network and cognitive radio. He delivered several invited lectures and made many expert appearances on various television channels and All India Radio. Dr. Bhattacharya is a member of The Institution of Electronics and Telecommunication Engineers, India and The Institution of Engineers, India. He received, in 2005, the Young Scientist Award from the International Union of Radio Science. He is working as a reviewer in many reputed journals, such as IEEE Journal on Selected Areas in Communications, IET Communications, Springer's IEIB, Elesevier's Computer Communication, Elsevier's Journal of Network and Computer Applications, Adhoc and Sensor Wireless Networks, Annals of Telecommunications – Annales des Télécommunications, Elsevier's Physical Communication, Indian Journal of Science and Technology etc. His name has been included in Marquis Who's Who in the World.

E-mail: hereispartha@gmail.com
Department of ECE, CET
Mody University of Science and Technology
Lakshmangarh – 332311, Rajasthan, India